Fermi National Accelerator Laboratory

FERMILAB-Pub-98/383-A

A New Limit on the Antiproton Lifetime

Stephen H. Geer and Dallas C. Kennedy

Fermi National Accelerator Laboratory
P.O. Box 500, Batavia, Illinois 60510

December 1998

Submitted to *Physical Review Letters*

Operated by Universities Research Association Inc. under Contract No. DE-AC02-76CH03000 with the United States Department of Energy

FERMILAB-PUB-98/383-A
UF-IFT-HEP-98-34

A NEW LIMIT ON THE ANTIPROTON LIFETIME

Stephen H. Geer*
Fermi National Accelerator Laboratory, P.O. Box 500, Batavia, Illinois 60510 USA

Dallas C. Kennedy**
Department of Physics, University of Florida, Gainesville, Florida 32611 USA
(December 1, 1998)

Measurements of the cosmic ray $\overline{p}/p$ ratio are compared to predictions from an inhomogeneous leaky disk model of $\overline{p}$ production and propagation within the galaxy, combined with a calculation of the modulation of the interstellar cosmic ray spectra as the particles propagate through the heliosphere to the Earth. The predictions agree with the observed $\overline{p}/p$ spectrum. Adding a finite $\overline{p}$ lifetime to the model, we obtain the limit $\tau_{\overline{p}} > 0.8$ Myr (90% C.L.).

98.70.Sa, 11.30.Er, 14.20.Dh

Submitted to **Physical Review Letters**

In recent years the presence of antiprotons ($\overline{p}$'s) in the cosmic ray (CR) flux incident upon the Earth has been firmly established by a series of balloon–borne experiments [1–10]. The measurements are summarized in Table 1. The observed CR $\overline{p}/p$ ratio has been shown to be in good agreement with predictions based on the Leaky Box Model (LBM) [11–13], which assumes that the $\overline{p}$'s originate from proton interactions in the interstellar (IS) medium. The $\overline{p}$'s then propagate within the Galaxy until they "leak out" with the characteristic CR Galactic storage time $T \sim 10$ million years (Myr) [14]. If the $\overline{p}$ lifetime $\tau_{\overline{p}}$ is not long compared to T the predicted $\overline{p}/p$ spectrum will be modified. The agreement of the LBM predictions with the observed $\overline{p}/p$ spectrum has therefore been used to argue that $\tau_{\overline{p}} > 10$ Myr [1,2,11]. This estimated limit is based on early CR $\overline{p}$ data, and does not take into account the reduction of the $\overline{p}$ decay rate due to time dilation, the effect of the heliosphere on the observed $\overline{p}/p$ spectrum, or the systematic uncertainties associated with the predictions. In this paper we compare recent CR data with the predictions of an improved LBM extended to permit a finite $\tau_{\overline{p}}$. Heliospheric corrections and systematic uncertainties are taken into account. Assuming a stable $\overline{p}$, we find excellent agreement between our predictions and the CR observations. Allowing the $\overline{p}$ to decay, we obtain a lower limit on $\tau_{\overline{p}}$ which is significantly more stringent than current laboratory bounds obtained from searches for $\overline{p}$ decay in ion traps [15] and storage rings [16]. The analysis presented in this paper improves on our earlier analysis [17] by including new data from ref. [10].

CPT invariance requires $\tau_{\overline{p}} = \tau_p$, where the proton lifetime τ_p is known to exceed $\mathcal{O}(10^{32})$ yr [18]. Although there is no compelling theoretical motivation to suspect a violation of CPT invariance, and hence a short $\overline{p}$ lifetime, it should be noted that string theories can accommodate CPT violation. Consider a dimension-6 CPT-violating operator with characteristic mass scale m_X. Dimensional analysis provides the estimate $\tau_{\overline{p}} \sim m_X^4/m_p^5$, yielding $m_X \sim (4.3 \times 10^9 \text{ GeV}) \times (\tau_{\overline{p}}/10 \text{ Myr})^{1/4}$. Hence, a search for $\overline{p}$ decay with a lifetime approaching 10 Myr provides a test for CPT violation well beyond the scale accessible at high energy colliders. Finally, since the antiproton is the only long lived antiparticle that could in principle decay into other known particles without violating charge conservation, a search for a modification of the CR $\overline{p}$ spectrum due to $\overline{p}$ decay provides a unique test of the stability of antimatter.

In the LBM the IS $\overline{p}$'s are assumed to be produced by the interactions of CR p's [11–13]: $pN_Z \to \overline{p}X$, where N_Z is a nucleus of charge Z, and X is anything. Our calculations use the elemental IS abundances given in refs. [12,13], and the measured cross sections for $Z = 1$ (the dominant contribution) given in ref. [11]. For $Z > 1$, we have used the "wounded nucleon" picture of [13]. The $\overline{p}$'s are assumed to propagate within the Galaxy until they are lost by either leakage into intergalactic space or by $p\overline{p}$ annihilation. The dominant loss process is leakage. Our analysis is based on the LBM of Gaisser and Schaeffer using the parameters of [13], but with a Galactic storage time improved to account for the non-uniform Galactic CR distribution [14]. This *inhomogeneous leaky disk model* (ILDM) results in a momentum dependent storage time $T(P) = (13 \text{ Myr}) \, [1 + P/(3 \text{ GeV})]^{-0.6}$.

The uncertainties on the parameters of the ILDM result in uncertainties on the normalization of the predicted $\overline{p}/p$ ratio but, to a good approximation, do not introduce significant uncertainties in the shape of the predicted spectrum. Uncertainties on four ILDM parameters must be considered: (i) the storage time ($\pm67\%$ [14]), (ii) the IS primary p flux ($\pm35\%$ [13]), (iii) the $\overline{p}$ production cross section ($\pm10\%$ [11,13]), and (iv) the composition of the IS medium, which introduces an uncertainty of $< 6\%$ on the predicted $\overline{p}$ flux [13]. We neglect the last of these uncertainties since it is relatively small. Within the quoted fractional uncertainties on the other three parameters we treat all values as being a priori equally likely. Note that the predicted $\overline{p}/p$ ratio is approximately proportional to each of the parameters under consideration.

The solid curves in Fig. 1 show the ILDM $\overline{p}/p$ spectra for the parameter choices that result in the largest and smallest $\overline{p}/p$ predictions. The predicted IS spectrum does not give a good description of the observed distribution at the top of the atmosphere. Good agreement is not expected because the CR spectra observed at the Earth are modulated as the particles propagate into the heliosphere [19,20], which consists of the solar magnetic field $\mathbf{B}$ and the solar wind. The wind, which is assumed to blow radially outwards, has a measured equatorial speed $V_W \sim 400$ km sec^{-1}. Away from the equatorial plane the *Ulysses* spacecraft has found $V_W \sim 750$ km sec^{-1} [21]. The wind also carries the solar magnetic flux outward. Solar rotation twists the field lines to form a Parker spiral. The smoothed heliomagnetic field ($B_\oplus \sim 5$ nT at the Earth's orbit) declines as it changes from radial at the Sun to azimuthal in the outer Solar System. The heliomagnetic polarity (sign(A)) is opposite in northern and southern solar hemispheres and switches sign somewhat after sunspot maximum (roughly every 11 years), when the field becomes more disordered. The regions of opposite magnetic polarity are separated by an approximately equatorial, unstable neutral current sheet. The sheet is wavy and spiraled; its waviness is measured by its "tilt" angle α, which relaxes from $\simeq 50^\circ$ at polarity reversal to $\lesssim 10^\circ$ just before reversal [19,21–23]. Cosmic rays enter the heliosphere on ballistic trajectories. The propagation of the CRs within the heliosphere is described by a drift-diffusion (Fokker-Planck) equation [24]. The CRs are pushed outwards by the bulk motion of the wind (elastic scattering), lose energy as they perform work on the wind (adiabatic deceleration or inelastic scattering), are diffusively scattered by field turbulence, and execute a drift *orthogonal* to the curving magnetic field lines as they spiral inwards *along* the field lines. Particles with $qA > 0$ (< 0) drift in along a polar (sheet) route. The IS particles with sufficient energy to overcome the various energy losses reach the inner Solar System with degraded momenta.

We compute the modulation of the CR fluxes by the method of characteristics and combined Runge-Kutta/Richardson-Burlich-Stoer techniques [25]. The calculation uses the heliospheric transport models of Jokipii *et al.* [23] updated by *Pioneer, Voyager, Helios, IMP* and *Ulysses* heliospheric measurements [26,21]. Our calculation includes magnetic curvature drift since older heliospheric models [27] that neglected this drift component have been shown [23] to be inadequate. The calculation is simplified by ignoring turbulence where its effects are small, which in practice means everywhere except across the sheet, where for particles with speed v the diffusion coefficient $\kappa_\perp = [(2-3)\times10^{17}\ \mathrm{m}^2/\mathrm{sec}][B_\oplus/B(r)](P/\mathrm{GeV})^{0.3}(v/c)$ is used. The effects of diffusion away from the sheet are expected to become significant for particles with kinetic energies < 300 MeV. In the following we restrict our analysis to the spectrum above 500 MeV to ensure that diffusion away from the sheet can be neglected.

We use the data sets recorded by the MASS91, IMAX, BESS, and CAPRICE experiments (Table 1). These data were recorded in the period 1991–1995, corresponding to a well–behaved part of the solar cycle for which the heliospheric modulation corrections can be confidently calculated. To explore the dependence of the predicted spectrum on the heliospheric parameters (equatorial V_W, polar V_W, and $B_\oplus$) we have computed the modulated spectra for 11 parameter sets (F1 - F11) that span the range of acceptable parameter values (Table 2). Using the central parameter values for our ILDM, and assuming a stable antiproton, the predicted modulated $\overline{p}/p$ spectra for a fixed time in the solar cycle (July 1995) are shown in Fig. 2 for each of the 11 heliospheric parameter sets. Figure 2 also shows the epoch-corrected measured CR spectra, obtained by multiplying each measurement by the factor $f \equiv R(\text{July 1995})/R(t)$, where $R(t)$ is the predicted $\overline{p}/p$ ratio at time t. The factors f, which are shown in Table 1 and have been computed using the F6 parameters, vary by up to ±0.06 with the parameter set choice. The predicted $\overline{p}/p$ spectra give an excellent description of the measurements. There is no evidence for an unstable $\overline{p}$.

To obtain a limit on $\tau_{\overline{p}}$ we add to the ILDM one additional loss mechanism, $\overline{p}$ decay. The results from maximum likelihood fits to the measurements are shown in Fig. 3 as a function of the assumed $\tau_{\overline{p}}$ for the 11 heliospheric parameter sets. The fits, which take account of the Poisson statistical fluctuations on the number of observed events and the background subtraction for each data set (Table 1), also allow the normalization of the ILDM predictions to vary within the acceptable range (Fig. 1). For a stable $\overline{p}$, at the 95% C.L. all of the heliospheric parameter sets yield predictions that give reasonable descriptions of the observed $\overline{p}/p$ spectrum. Allowing for a finite $\tau_{\overline{p}}$, the heliospheric parameter sets with larger wind speeds permit lower $\overline{p}$ lifetimes. This can be understood by noting that, as the wind speed increases, the predicted flux of polar–routed particles (protons in the present solar cycle) is depleted at low energies, which increases the predicted $\overline{p}/p$ ratio. Antiproton decay would compensate for this distortion in the predicted spectrum. Hence our fits using the extreme parameter set F11 determine the limits on $\tau_{\overline{p}}$. We obtain the bounds:

$$\tau_{\overline{p}} \quad > \quad 0.8 \text{ Myr} \ \ (90\% \text{ C.L.}) \quad , \quad 0.7 \text{ Myr} \ \ (95\% \text{ C.L.}) \quad , \quad 0.5 \text{ Myr} \ \ (99\% \text{ C.L.}) \quad . \tag{1}$$

These limits are significantly more stringent than those obtained from the most sensitive laboratory search for inclusive $\overline{p}$ decay ($\tau_{\overline{p}} > 3.4$ months [15]) or the most sensitive search for an exclusive $\overline{p}$ decay mode ($\tau_{\overline{p}}/B(\overline{p} \to \mu^- \gamma) >$ 0.05 Myr [16]). Our simple dimensional analysis suggests that if antiprotons do decay due to a CPT–violating coupling, the mass scale at which this new physics takes place exceeds $\mathcal{O}(10^8)$ GeV/c^2.

Acknowledgments

It is a pleasure to thank Thomas Gaisser, J. R. Jokipii, and E. J. Smith for their insights. This work was supported at Fermilab under grants U.S. DOE DE-AC02-76CH03000 and NASA NAG5-2788. and at the U. Florida, Institute for Fundamental Theory, under grant U.S. DOE DE-FG05-86-ER40272.

---

* E-mail: sgeer@fnal.gov.
** E-mail: kennedy@phys.ufl.edu.

[1] R.L. Golden *et al., Phys. Rev. Lett.* **43**, 1196 (1979).
[2] E.A. Bogomolov *et al., Proc.* 16^{th} *ICRC, Kyoto* **1**, 330 (1979).
[3] E.A. Bogomolov *et al., Proc.* 20^{th} *ICRC, Moscow* **2**, 72 (1987).
[4] E.A. Bogomolov *et al., Proc.* 21^{st} *ICRC, Adelaide* **3**, 288 (1990).
[5] M. Hof *et al., Astrophys. J.* **467**, L33 (1996).
[6] J.W. Mitchell *et al., Phys. Rev. Lett.* **76**, 3057 (1996).
[7] A. Moiseev *et al., Astrophys. J.* **474**, 479 (1997).
[8] K. Yoshimura *et al., Phys. Rev. Lett.* **75**, 3792 (1995).
[9] M. Boezio *et al., Astrophys. J.* **487**, 415 (1997).
[10] H. Matsunaga *et al., Phys. Rev. Lett.* **81**, 4052 (1998).
[11] S. A. Stephens, *Astrophys. Space Sci.* **76**, 87 (1981); S. A. Stephens and R. L. Golden, *Space Sci. Rev.* **46**, 31 (1987).
[12] W. R. Webber and M. S. Potgieter, *Astrophys. J.* **344**, 779 (1989).
[13] T. K. Gaisser and R. K. Schaefer, *Astrophys. J.* **394**, 174 (1992).
[14] W. R. Webber *et al., Astrophys. J.* **390**, 96 (1992); P. Chardonnet *et al., Phys. Lett.* **B384**, 161 (1996).
[15] G. Gabrielse *et al.* (Antihydrogen Trap Collab.), CERN proposal CERN-SPSLC-96-23 (1996).
[16] S. Geer *et al., Phys. Rev. Lett.* **72**, 1596 (1994); M. Hu *et al.* (APEX Collab.), *Phys. Rev.* **D58**, 111101 (1998).
[17] S. Geer and D.C. Kennedy, astro-ph/9809101 (1998), unpublished.
[18] C. Caso *et al.* (Particle Data Group), *Euro. Phys. J.* **C3**, 613 (1998).
[19] M. Stix, *The Sun: An Introduction* (Berlin: Springer-Verlag, 1989); T. Encrenaz *et al., The Solar System,* 2nd ed. (Berlin: Springer-Verlag, 1990); R. Howard, *Ann. Rev. Astron. Astrophys.,* **22**, 131 (1984). The wavy sheet's locus in polar coordinates is $\cos\theta + \sin\alpha \cdot \sin[\varphi + \Omega_\odot r/V_W] = 0$.
[20] M. S. Longair, *High Energy Astrophysics,* 2 vols., 2nd ed. (Cambridge: Cambridge University Press, 1992).
[21] E. J. Smith, R. G. Marsden *et al., Science* **268**, 1005ff. (1995); J. Kóta and J. R. Jokipii, ibid., 1024; R. G. Marsden, E. J. Smith *et al., Astron. Astrophys.* **316**, 279ff. (1996); Ulysses http://ulysses.jpl.nasa.gov/ .
[22] National Solar Observatory http://www.nso.noao.edu/pub/sunspots .
[23] J. R. Jokipii and D. A. Kopriva, *Astrophys. J.* **234**, 384 (1979); J. R. Jokipii and P. A. Isenberg, *Astrophys. J.* **234**, 746 (1979); **248**, 845 (1981); J. R. Jokipii and B. Thomas, *Astrophys. J.* **243**, 1115 (1981); J. R. Jokipii and J. M. Davila, *Astrophys. J.* **248**, 1156 (1981).
[24] H. Risken, *The Fokker-Planck Equation: Methods of Solution and Applications* (New York: Springer-Verlag, 1984).
[25] E. C. Zachmanoglou and D. W. Thoe, *Introduction to Partial Differential Equations with Applications* (New York: Dover Publications, 1986); W. H. Press *et al., Numerical Recipes in C: The Art of Scientific Computing,* 2nd ed. (Cambridge: Cambridge University Press, 1992).
[26] See http://nssdc.gsfc.nasa.gov/space/ and http://www.sec.noaa.gov/ .
[27] L. J. Gleeson and W. I. Axford, *Astrophys. J.* **149**, L115 (1967); *Astrophys. J.* **154**, 1011 (1968); L. A. Fisk and W. I. Axford, *J. Geophys. Res.* **74**, 4973 (1969); L. A. Fisk, *J. Geophys. Res.* **76**, 221 (1971).

Experiment		Field Pol.	Flight Date	f	KE Range (GeV)	Cand-idates	Back-ground	Observed $\overline{p}/p$ Ratio	predict-tion
Golden†	[1]	+	June 1979	–	5.6 – 12.5	46	18.3	$(5.2 \pm 1.5) \times 10^{-4}$	-
Bogomolov†	[2]	+	1972-1977	–	2.0 – 5.0	2	-	$(6 \pm 4) \times 10^{-4}$	-
Bogomolov‡	[3]	−	1984-1985	–	0.2 – 2.0	1	-	$(6^{+14}_{-5}) \times 10^{-5}$	-
Bogomolov‡	[4]	−	1986-1988	–	2.0 – 5.0	3	-	$(2.4^{+2.4}_{-1.3}) \times 10^{-4}$	-
MASS91	[5]	+	Sep. 1991	1.1	3.70-19.08	11	3.3	$(1.24^{+0.68}_{-0.51}) \times 10^{-4}$	1.3×10^{-4}
IMAX‡	[6]	+	July 1992	–	0.25 – 1.0	3	0.3	$(3.14^{+3.4}_{-1.9}) \times 10^{-5}$	1.5×10^{-5}
IMAX	[6]	+	July 1992	0.96	1.0 – 2.6	8	1.9	$(5.36^{+3.5}_{-2.4}) \times 10^{-5}$	6.5×10^{-5}
IMAX	[6]	+	July 1992	1.1	2.6 – 3.2	5	1.2	$(1.94^{+1.8}_{-1.1}) \times 10^{-4}$	1.1×10^{-4}
BESS93‡	[7]	+	July 1993	–	0.20 – 0.60	7	~ 1.4	$(5.2^{+4.4}_{-2.8}) \times 10^{-6}$	8.9×10^{-6}
CAPRICE	[9]	+	Aug. 1994	0.94	0.6 – 2.0	4	1.5	$(2.5^{+3.2}_{-1.9}) \times 10^{-5}$	3.5×10^{-5}
CAPRICE	[9]	+	Aug. 1994	1.0	2.0 – 3.2	5	1.3	$(1.9^{+1.6}_{-1.0}) \times 10^{-4}$	1.1×10^{-4}
BESS95‡*	[10]	+	July 1995	1.0	0.175 – 0.3	3	0.17	$(7.8^{+8.3}_{-4.8}) \times 10^{-6}$	−
BESS95‡*	[10]	+	July 1995	1.0	0.3 – 0.5	7	0.78	$(7.4^{+4.7}_{-3.3}) \times 10^{-6}$	1.1×10^{-5}
BESS95*	[10]	+	July 1995	1.0	0.5 – 0.7	7	1.4	$(7.7^{+5.3}_{-3.7}) \times 10^{-6}$	5.5×10^{-6}
BESS95*	[10]	+	July 1995	1.0	0.7 – 1.0	11	2.8	$(1.01^{+5.7}_{-4.3}) \times 10^{-5}$	1.3×10^{-5}
BESS95*	[10]	+	July 1995	1.0	1.0 – 1.4	15	3.5	$(1.99^{+0.91}_{-0.73}) \times 10^{-5}$	3.1×10^{-5}

TABLE I. Summary of cosmic ray antiproton results. Listed from left to right are: experiment, solar cycle polarity, balloon flight date, epoch correction factor, $\overline{p}$ kinetic energy range, number of $\overline{p}$ candidates observed, estimated number of background events, measured $\overline{p}/p$ ratio at the top of the atmosphere, and the ILDM prediction using the F6 heliospheric parameters. † Not shown in Fig. 1 or used in analysis. ‡ Not used in analysis. * Statistical and systematic uncertainties on ratio added in quadrature.

Set	Equatorial V_W (km sec^{-1})	Polar V_W (km sec^{-1})	$B_\oplus$ (nT)
F1	375	700	4.0
F2	380	710	4.1
F3	385	720	4.2
F4	390	730	4.3
F5	395	740	4.4
F6	400	750	4.5
F7	405	760	4.6
F8	410	770	4.7
F9	415	780	4.8
F10	420	790	4.9
F11	425	800	5.0

TABLE II. Heliospheric parameter sets.

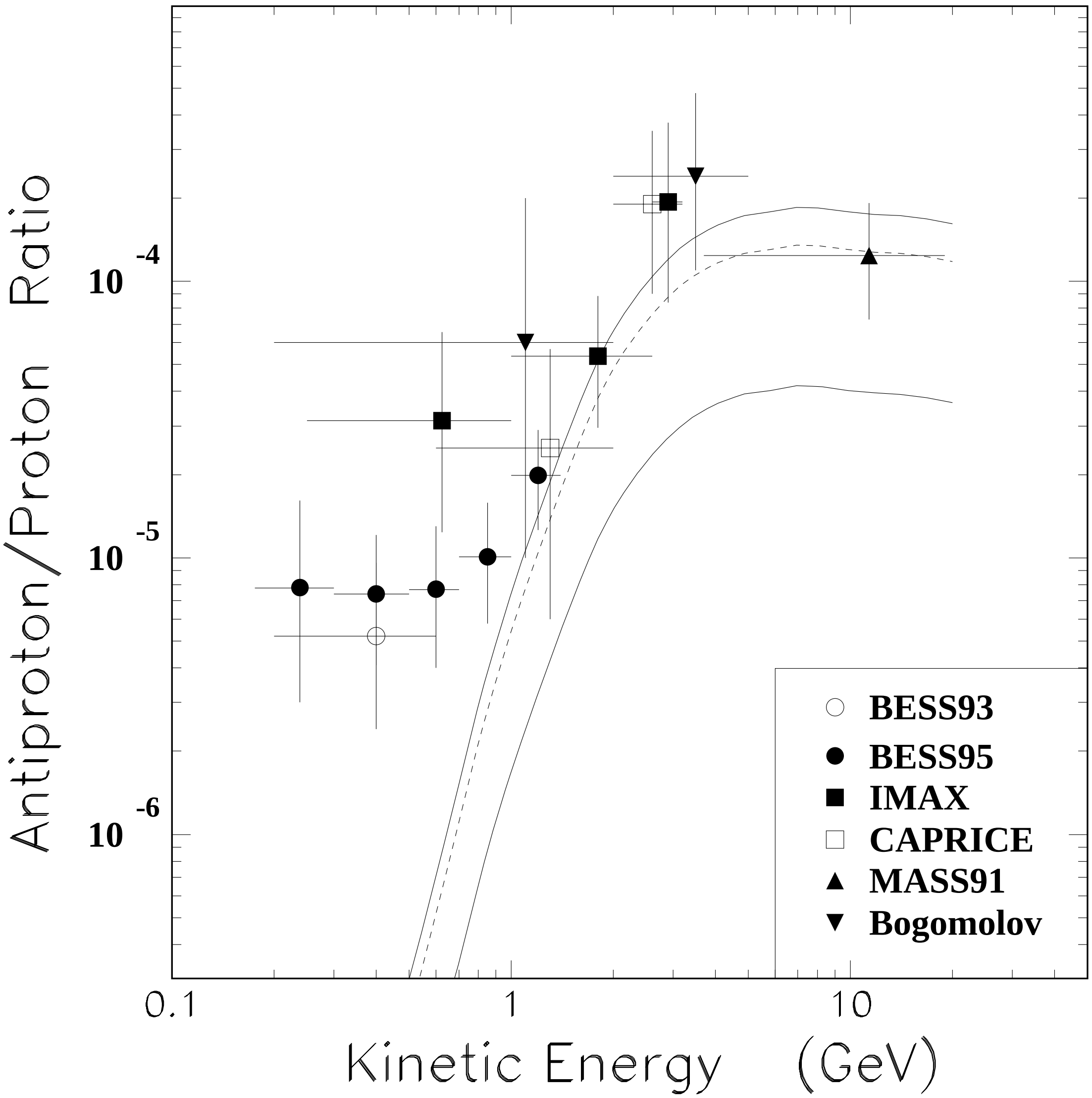

FIG. 1. Observed $\overline{p}/p$ ratio at the top of Earth atmosphere (see Table 1). The solid curves show the upper and lower interstellar ratios predicted by the ILDM described in the text, without solar modulation. The broken curve shows the ILDM prediction with the same parameters used for the modulated predictions of Fig. 2.

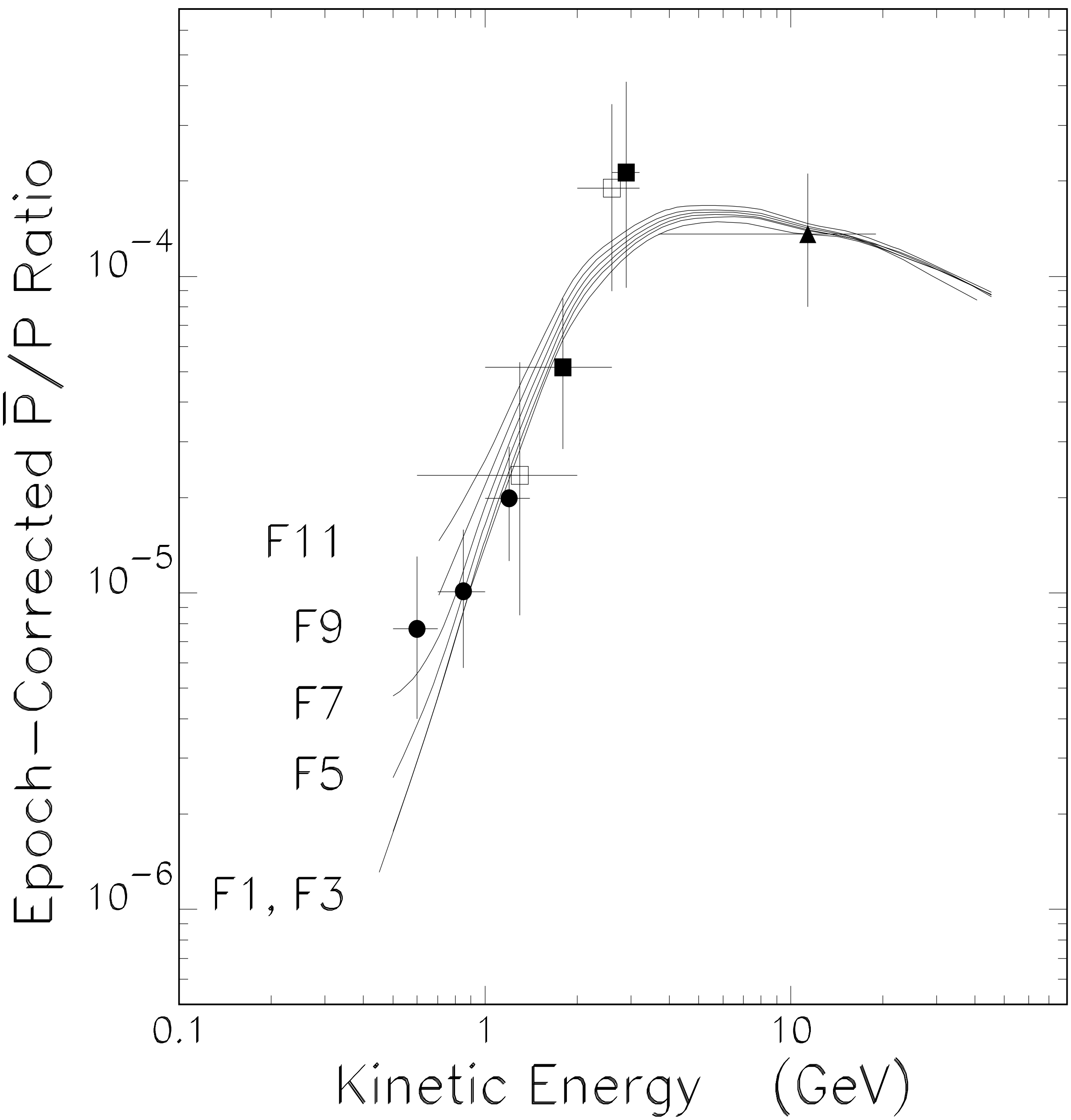

FIG. 2. Observed $\overline{p}/p$ spectrum (kinetic energy > 500 MeV) at the top of the atmosphere compared with the ILDM predictions (see broken curve on Fig. 1) after modulation using the heliospheric parameter sets indicated (see Table 2). The curves are predictions for the spectrum observed in July 1995. The data have been corrected to correspond to this epoch (see text).

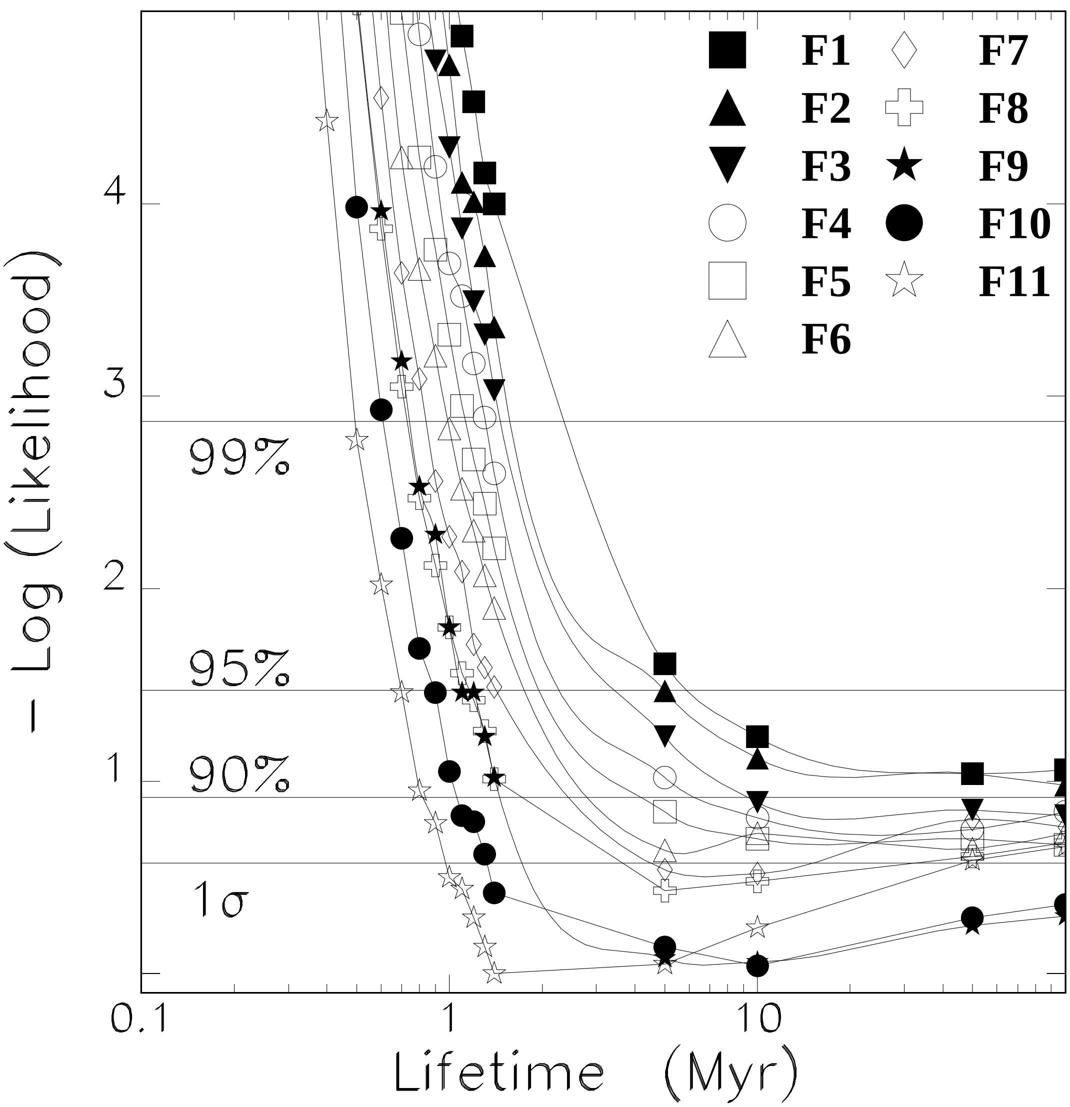

FIG. 3. Fit results as a function of the assumed $\tau_{\overline{p}}$ for the eleven heliospheric parameter sets (F1 – F11) shown in Table 2.